IEEE Access
Multidisciplinary | Rapid Review | Open Access Journal

Received 31 May 2023, accepted 20 June 2023, date of publication 23 June 2023, date of current version 28 June 2023.

Digital Object Identifier 10.1109/ACCESS.2023.3289074

RESEARCH ARTICLE

Circularly Polarized Wideband Uniplanar Crossed-Dipole Antenna With Folded Striplines and Rectangular Stubs

HEESU WANG[1], (Graduate Student Member, IEEE), GANGIL BYUN[2], (Senior Member, IEEE), YONG BAE PARK[1,3], (Senior Member, IEEE), AND IKMO PARK[1], (Member, IEEE)

[1]Department of Electrical and Computer Engineering, Ajou University, Suwon 16499, South Korea
[2]Department of Electrical Engineering, Ulsan National Institute of Science and Technology, Ulsan 44919, South Korea
[3]Department of AI Convergence Network, Ajou University, Suwon 16499, South Korea

Corresponding author: Ikmo Park (ipark@ajou.ac.kr)

This work was supported in part by the National Research Foundation of Korea (NRF) Grant funded by the Korean Government [Ministry of Science and ICT (MSIT)] under Grant NRF-2022R1F1A1065324 and Grant 2021R1A4A1030775; and in part by the Institute of Information and Communications Technology Planning and Evaluation (IITP) Grant funded by the Korea Government (MSIT), Development of 3D-NET Core Technology for High-Mobility Vehicular Service, under Grant 2022-0-00704-001.

ABSTRACT A circularly polarized (CP) wideband uniplanar crossed-dipole antenna is presented in this paper. The antenna constitutes a pair of identical crossed-dipole arms printed on the same plane of a dielectric substrate. Each crossed-dipole component is a pair of thin dipole arms that are perpendicular to each other and connected with a folded stripline for generating CP radiations. A pair of thin rectangular stubs are introduced on one dipole arm at the center of the antenna to improve impedance-matching bandwidth. Another set of rectangular stubs is attached at the sides of the dipole arms to broaden the axial ratio (AR) bandwidth. The antenna in free space is excited via a coaxial probe with a balun. It generates two adjacent AR bands that are merged into a wide AR bandwidth with bidirectional radiation patterns. Full-wave electromagnetic simulations are performed in the design process, and experiments are performed to validate the antenna design. The proposed antenna sized 42.4 mm $\times$ 42.4 mm $\times$ 0.2032 mm (0.57 λ_o $\times$ 0.57 λ_o $\times$ 0.0027 λ_o at 4.05 GHz) has an $|S_{11}| < -10$ dB impedance bandwidth of 2.92–5.15 GHz (55.26%) and a 3 dB AR bandwidth of 2.96–5.12 GHz (53.5%).

INDEX TERMS Compact antenna, crossed dipole, circular polarization, uniplanar, wideband.

I. INTRODUCTION

Circularly polarized (CP) antennas possess many advantages over linearly polarized antennas, such as enhanced immunity to multipath distortion, polarization mismatch losses, and Faraday rotation effects caused by the ionosphere. Owing to these superior qualities, the demand for CP antennas has grown immensely in wireless communication applications [1], [2], [3], [4], [5], [6], [7], [8], [9], [10], [11], [12]. In particular, crossed-dipole antennas have attracted considerable interest owing to their excellent CP characteristics, simple structure, compact size, and flexible shape [13], [14], [15], [16], [17], [18], [19], [20], [21], [22], [23], [24], [25], [26], [27], [28], [29], [30], [31], [32]. Notably, traditional crossed-dipole antennas, which are composed of thin dipole elements, offer limited bandwidths [16], [17], [18], [19], [20], [21]. The demands of increasing bandwidth in modern wireless communication systems and progression in antenna design have prompted the development of wideband crossed-dipole antennas [22], [23], [24], [25], [26], [27], [28], [29], [30], [31], [32], [33], [34], [35]. Recently, several techniques have been developed to widen the axial ratio (AR) bandwidth of crossed-dipole antennas. A common approach for achieving a wide AR bandwidth with a

The associate editor coordinating the review of this manuscript and approving it for publication was Hassan Tariq Chattha.

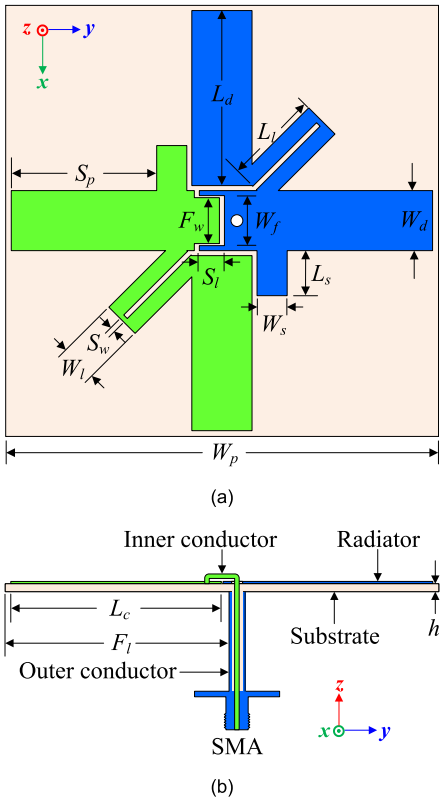

FIGURE 1. Geometry of crossed-dipole antenna: (a) top view and (b) side view.

crossed-dipole antenna is to substitute thin linear dipoles with wide planar dipoles, such as fat dipoles [22], [23], stepped dipoles [24], [25], and bowtie dipoles [26], [27]. Other approaches to increase the bandwidth include the incorporation of additional radiators, such as parasitic elements around the crossed dipole [28], [29], [30]. Overall, effective bandwidth enhancement can be achieved by combining wide planar crossed dipoles and parasitic elements [31], [32], [33], [34], [35]. However, the use of additional radiators with large sizes can increase the device size and fabrication cost. Furthermore, the complex structures of these antennas may limit large-scale production.

To address these problems, we developed a CP wideband uniplanar crossed-dipole antenna. The proposed antenna is composed of a pair of identical thin crossed-dipole arms printed on the same plane of a dielectric substrate. In the proposed framework, the antenna design and fabrication complexities are lower than those of traditional crossed-dipole antennas with vacant-quarter printed rings that use both sides of the substrate. One pair of stubs and one pair of folded striplines were placed near the center of the crossed dipole to improve impedance matching and generate circular polarization. To widen the AR bandwidth of the antenna, the first- and third-order modes of the antenna are compressed by adding rectangular stubs to the dipole in the y-direction. The antenna was optimized with a series of ANSYS High-Frequency Simulation Software (HFSS) simulations. The performance characteristics of the proposed antenna with an overall size of 42.4 mm × 42.4 mm × 0.2032 mm (0.57 λ_o × 0.57 λ_o × 0.0027 λ_o at 4.05 GHz) could be summarized as follows: $|S_{11}| < -10$ dB bandwidth of 2.92–5.15 GHz (55.26%), 3 dB AR bandwidth of 3.0–5.09 GHz (51.7%), and peak gain of 2.08 dBic at 4.15 GHz. The antenna radiation efficiency within the bandwidth is more than 93%.

II. ANTENNA GEOMETRY AND DESIGN

Fig. 1 shows the geometry of the uniplanar crossed-dipole antenna, which consists of crossed dipoles, a dielectric substrate, a coaxial feedline, and a 50-Ω SMA connector. The dielectric substrate material is Rogers RO4003, which has a dielectric constant of $\varepsilon_r = 3.38$ and loss tangent of $tan\delta = 0.0027$. Both arms of the crossed dipole are printed on the top side of the same plane in the dielectric substrate and directly fed by a coaxial line with the 50-Ω SMA connector. The antenna is fed by a coaxial cable slightly displaced to one side along the y-axis, the outer conductor attached to one crossed-dipole arm, and the inner conductor passing through the same arm without any contact with the other crossed-dipole arm. A pair of thin rectangular stubs are installed at one of the y-axis arms near the center of the antenna for impedance matching.

The uniplanar crossed-dipole antenna was optimized with a series of HFSS simulations to ensure satisfactory impedance matching with the 50-Ω coaxial feedline and to merge the two adjacent AR bands into a wide AR bandwidth. The optimized design parameters were set as follows: $W_p = 42.4$ mm, $L_d = 18$ mm, $L_c = 20.95$ mm, $W_d = 6$ mm, $L_l = 9$ mm, $W_l = 3.3$ mm, $S_w = 0.1$ mm, $L_s = 4.5$ mm, $W_s = 3$ mm, $S_p = 14.5$ mm, $F_w = 5.6$ mm, $W_f = 5.8$ mm, $F_l = 22.5$ mm, $S_l = 3.5$ mm, and $h = 0.2032$ mm.

The crossed dipoles are composed of two dipole arms that are orthogonal to each other. CP radiation is generated when the real parts of the input admittances of the dipoles are equal, and the phase angles of their input admittances differ by 90° [6]. The input admittance of the dipole constituting the crossed-dipole antenna must be constant in a wide frequency range to implement a CP crossed-dipole antenna with a wide AR bandwidth. To realize a wideband dipole, the first- and third-order modes of the dipole are compressed by adding a rectangular stub structure to the y-axis of the dipole arms [36], [37], [38]. Fig. 2 shows the structure of a stub-loaded uniplanar mode compressed dipole. Fig. 3 shows the variation of the reflection coefficient according to the stub length of the stub-loaded uniplanar dipole. The simulation results in Fig. 3 clearly show that the length of the dipole (L_d) determines the frequency of the first resonant mode and that the length of the stub (L_s) determines the frequency of the second resonant mode. Fig. 4 shows the antenna surface current distribution in each resonant mode. Fig. 4(a) shows the dipole surface current distribution at 3.5 GHz, the first resonant mode, and shows that the dipole operates in the first-order mode. Fig. 4(b) shows the surface current

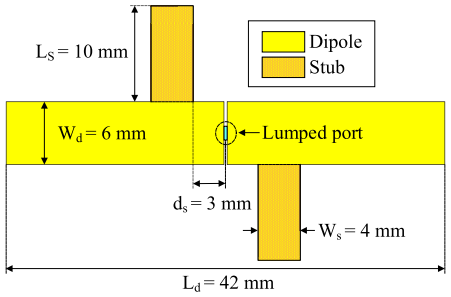

FIGURE 2. Geometry of the stub-loaded uniplanar dipole antenna.

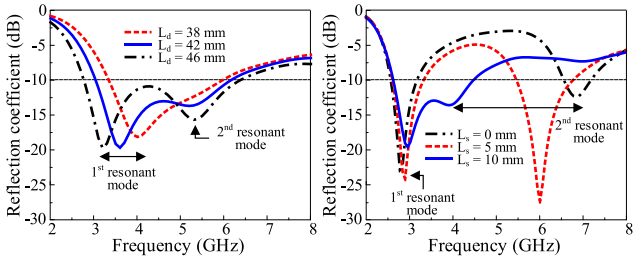

FIGURE 3. Effect of dipole length and stub length: (a) dipole length (L_d) and (b) stub length (L_s).

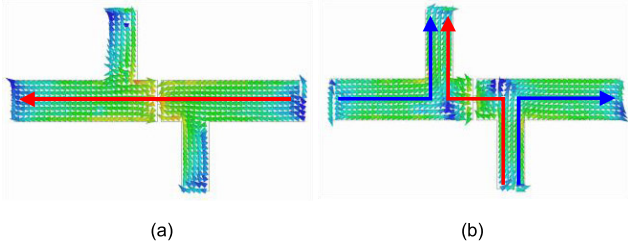

FIGURE 4. Current distributions of the stub-loaded dipole: (a) 3.5 GHz and (b) 5.2 GHz.

distribution at 5.2 GHZ, the second resonant mode, and shows that the dipole operates in the third-order mode at that frequency.

A crossed dipole with wideband characteristics consists of a stub-loaded uniplanar mode compression dipole and a pair of striplines are folded to connect the two perpendicular dipole arms to satisfy the CP generation condition. The uniplanar crossed-dipole antenna exhibits wideband performance characteristics in terms of impedance and AR bandwidths. The reflection coefficient profile of the antenna exhibits two resonances at 3.5 GHz and 4.9 GHz. The impedance bandwidth is 2.25 GHz (2.84–5.09 GHz), corresponding to a fractional equivalent bandwidth of 56.75%. The antenna produces two AR bands corresponding to the AR minimum points at 3.2 GHz and 4.6 GHz. The adjacent bands are merged to achieve a wide AR bandwidth of 2.03 GHz (2.98–5.01 GHz), corresponding to a fractional equivalent bandwidth of 50.81%.

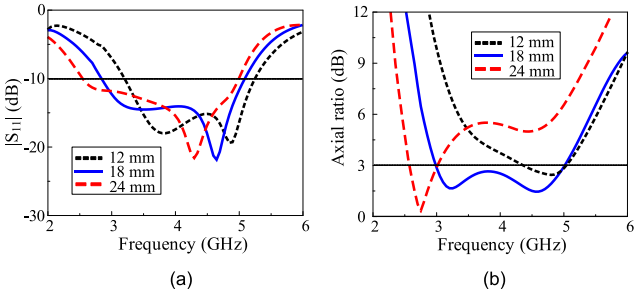

FIGURE 5. Effects of dipole length (L_d): (a) reflection coefficient and (b) axial ratio.

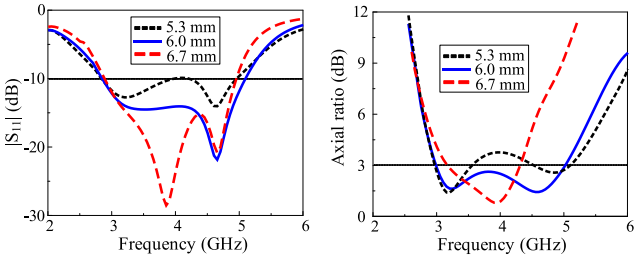

FIGURE 6. Effects of dipole width (W_d): (a) reflection coefficient and (b) axial ratio.

III. PARAMETRIC STUDY

Parametric studies were performed on the proposed CP unipolar crossed-dipole antenna to clarify the operation principle and influence of the antenna parameters on the antenna performance. Only one parameter was varied while the other parameters were maintained at their optimum values, and the effects on the reflection coefficient and AR were noted.

First, the effects of the dipole parameters, i.e., the dipole length (L_d) and width (W_d), are discussed. The dipole length is a key parameter in antenna design because it determines the resonant frequency, and it must be appropriately adjusted to achieve the desired frequency of operation. Changes in the dipole length result in shifting the reflection coefficient ($|S_{11}|$) curve along the frequency scale. For example, when the length increases, the $|S_{11}|$ curve moves toward low frequencies while retaining a similar impedance bandwidth, as shown in Fig. 5(a). In addition, the dipole lengths influence the generation of the first AR band at low frequencies. As the dipole length changes, the first AR band at a low frequency moves along the frequency scale, whereas the other AR band at a high frequency retains its position, as shown in Fig. 5(b). This finding indicates that changes in the dipole lengths affect the resonant frequency of the antenna and first AR band. The dipole width has dual functions of impedance matching and AR broadening in antenna design. The impedance matching of the antenna is enhanced and deteriorated as the dipole width increases and decreases, respectively, as shown in Fig. 6(a), which highlights the role of the dipole width in impedance matching. As shown in Fig. 6(b), the second AR band shifts toward lower and higher frequencies as the dipole

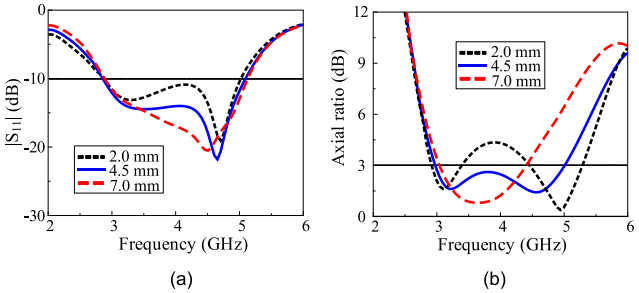

FIGURE 7. Effects of AR stub length (L_s): (a) reflection coefficient and (b) axial ratio.

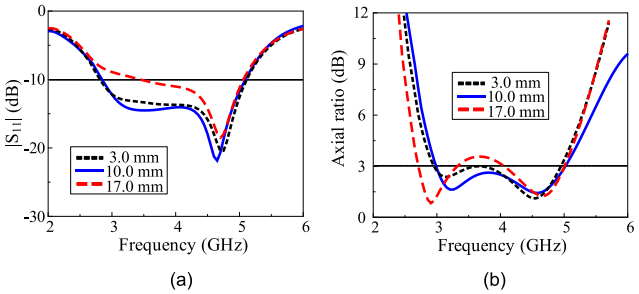

FIGURE 8. Effects of AR stub width (W_s): (a) reflection coefficient and (b) axial ratio.

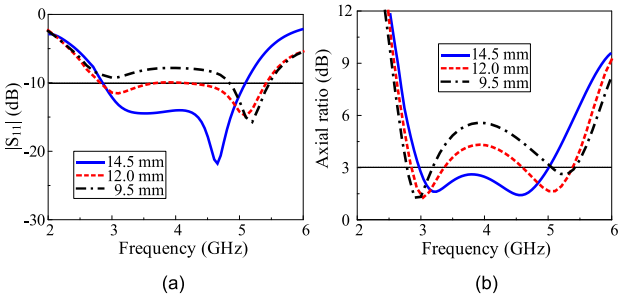

FIGURE 9. Effects of AR stub position (S_p): (a) reflection coefficient and (b) axial ratio.

width increases and decreases, respectively. In particular, as the dipole width varies, the real part and phase angle of the input admittance of the dipole change, leading to variations in the second AR minimum point. In other words, the dipole widths can be modified to allow the second AR band to merge into a wide AR bandwidth.

Next, the effects of the AR stub parameters, i.e., the length (L_s), width (W_s) and position (S_p), are explored. The effect of the AR stub length on the AR is more notable than that on the reflection coefficient. In particular, variations in the AR stub length lead to insignificant changes in the reflection coefficient and impedance matching, as shown in Fig. 7(a). In particular, the AR stub length is an essential parameter as its changes cause the second AR minimum point at high frequencies to shift considerably along the frequency scale, as shown in Fig. 7(b). Therefore, the AR stub and dipole width influence the introduction of a second AR band by altering the input admittance of the dipoles to produce phase angles that differ by 90° and real parts that are equal in magnitude and generate another AR band at high frequencies. The width of the AR stub (Fig. 8(a)) does not considerably influence the reflection coefficient. An increase in the AR stub width causes the impedance matching to degrade, particularly at lower frequencies. Therefore, small AR stub widths are required to match the antenna at lower frequencies. Small AR stub widths do not lead to significant changes in the AR and AR bandwidth. However, a large AR stub width shifts the first AR band toward lower frequencies, as shown in Fig. 8(b). In particular, when the AR stub widths are large, the dipole size increases, which shifts the first AR band toward lower frequencies because the AR stubs are attached along the dipole length. AR Fig. 9 shows the effect of the AR stub position. As the AR stub moves to the edge of the dipole, the dipole behaves similarly to a bent dipole, causing the antenna's first resonant mode frequency to be lower and the second resonant mode frequency to be higher. Fig. 9(a) shows the reflection coefficient according to the position of the AR stub, and as the AR stub moves to the edge of the dipole, the first resonant mode frequency decreases and the second resonant mode frequency increases. In Fig. 9(b), the AR is displayed according to the AR stub position. A CP crossed-dipole antenna produces circular polarization when the input conductance of each dipole element is the same, and the input admittance phase angle difference is 90°. As the AR stub moves toward the edge of the dipole, the first resonant mode frequency decreases, and the second resonant mode frequency increases. Hence, as the AR stub moves, the first AR minimum point frequency decreases and the second AR minimum point frequency increases.

Finally, the effects of folded stripline parameters, i.e., the length (L_l) and width (W_l), are examined. The stripline length affects the impedance matching and AR of the antenna, as shown in Fig. 10(a). In the case of small stripline lengths, the antenna exhibits satisfactory impedance matching with the wide impedance bandwidth. In contrast, as the stripline length increases, the impedance matching deteriorates, and the impedance bandwidth narrows. Furthermore, the stripline length considerably affects the AR and AR bandwidth, as shown in Fig. 10(b). At the optimum stripline length, the AR curve exhibits two AR bands that merge into a wide AR bandwidth. When the stripline length is smaller than the optimal value, the AR deteriorates, the high-frequency AR band disappears, and only the low-frequency AR band remains. When the stripline length is larger than the optimal value, the AR increases, although all the AR bands are retained. The reflection coefficient and impedance bandwidth are only slightly affected by the stripline width, as shown in Fig. 11(a). When the stripline width increases to more than the optimal value, the impedance matching deteriorates, and the impedance bandwidth decreases marginally. In terms of the AR and AR bandwidth, the stripline width more notably influences the AR than the reflection coefficient. Fig. 11(b) shows that the AR gradually worsens as the

TABLE 1. Performance comparison of the proposed antenna with other CP antenna designs.

Antenna structure	Size (λ^3)	f_c (GHz)	IBW (%)	AR BW (%)	Rad. type	Peak gain (dBic)	Eff. (%)
Ref [9][1]	0.445× 0.445× 0.006	1.6	31.9	21.56	B	5.0	90
Ref [10][2]	0.68× 0.68× 0.18	1.58	52.4	7.55	U	7.7	-
Ref [18][1]	0.37× 0.37× 0.0055	3.25	16.4	11.7	B	1.9	93
Ref [25][1]	2.414× 0.675× 0.16	27	34.6	23.1	U	8.8	-
Ref [34][1]	0.46× 0.46× 0.17	5.85	40.8	22.03	U	6.5	88
Ref [35][1]	0.35× 0.35× 0.0031	1.5	30.4	20.5	B	1.9	80
Proposed design[1]	0.57× 0.57× 0.0027	4.04	55.26	53.5	B	2.08	93

IBW: impedance bandwidth. AR BW: axial ratio bandwidth.
B: Bi-directional. U: Uni-directional
λ: center frequency of 3-dB AR bandwidth
[1]$|S_{11}| \leq -10$ dB, [2]$|S_{11}| \leq -15$ dB

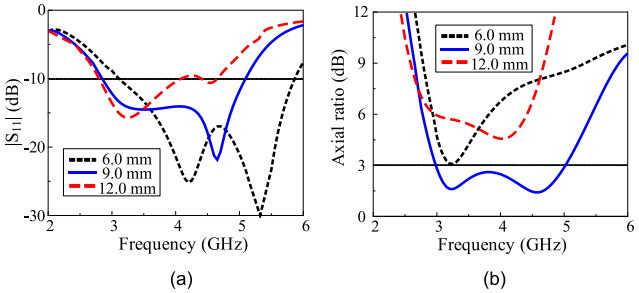

FIGURE 10. Effects of folded stripline length (L_l): (a) reflection coefficient and (b) axial ratio.

stripline width increases to more than the optimal value. The AR worsening is accompanied with the disappearance of one of the AR bands and a decrease in the AR bandwidth. Therefore, the stripline width must be appropriately set to achieve impedance matching and generate a wide AR bandwidth.

When a coaxial cable is used to feed the dipole antenna, the characteristics of the antenna change because of the leakage current [39]. The leakage current of the coaxial cable can be decreased using a balun. In this study, a quarter wavelength balun was designed and attached to the coaxial cable to prevent the leakage current, which causes poor radiation patterns. The balun extended 21 mm along the coaxial cable, and the cable was connected to the outer conductor at the bottom of the balun to eliminate the common mode current from flowing over the outer conductor of the coaxial cable to avoid radiation pattern distortion and eliminate the fluctuation in the gain. The introduction of the balun was expected

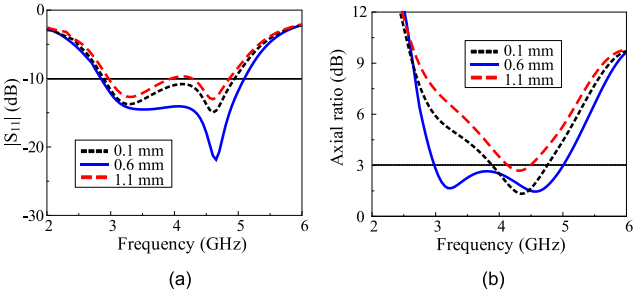

FIGURE 11. Effects of folded stripline width (S_w): (a) reflection coefficient and (b) axial ratio.

to vary the antenna performance characteristics in terms of the reflection coefficient and AR. Therefore, the antenna with a balun was re-optimized with the following design parameters: $W_p = 42.4$ mm, $L_d = 17.5$ mm, $L_c = 20.8$ mm, $W_d = 6$ mm, $L_l = 7.5$ mm, $W_l = 3.3$ mm, $S_w = 0.1$ mm, $L_s = 4.5$ mm, $W_s = 5$ mm, $S_p = 12.5$ mm, $F_w = 5.6$ mm, $W_f = 5.8$ mm, $F_1 = 22.7$ mm, $S_l = 1$ mm, and $h = 0.2032$ mm. Table 1 compares the proposed unipolar crossed-dipole antenna with other CP dipole antennas, in terms of the antenna size, impedance bandwidth, AR bandwidth, gain, and radiation efficiency. A sequentially rotated dipole array antenna using a crossed-dipole structure as a feed network has been described previously [9]. The gain is high as the four dipoles operate sequentially to generate circular polarization. However, the AR bandwidth is not wide because the bandwidth of the dipole constituting the antenna is narrow. A circularly polarized multi-dipole antenna using dipoles of different lengths has also been described [10]. The antenna consists of two pairs of dipoles with different lengths, and circular polarization is generated by the input admittance phase angle difference of each pair of dipoles. The AR bandwidth is very narrow because a narrow dipole is used. In addition, a folded E-shaped crossed dipole has been reported [18]. After rotating the upper structure of the biplanar crossed dipole by 90° around the feed point and bending each dipole arm, a step structure was applied to the phase delay line to miniaturize the antenna. This antenna has a smaller size than that of a conventional crossed-dipole antenna but has a limited AR bandwidth. An antenna that implements an additional resonant mode using a complex-shaped dipole has been reported [25]. A zigzag structure was applied to the edge of the dipoles to realize a wide impedance bandwidth, and the corners of each dipole arm were cut off to widen the AR bandwidth. However, despite its complex shape, the bandwidth of the antenna is not very wide. Furthermore, an antenna in which parasitic elements operating as a magneto-electric dipole were added to a crossed-dipole antenna has been described [34]. In this study, a crossed dipole with an Egyptian axe dipole was used to reduce the size of the antenna, and four patches connected with a ground plane by metal pins were added for an additional resonant mode. As the bandwidth of the crossed dipole itself is narrow, the bandwidth of the antenna is not wide, despite the addition

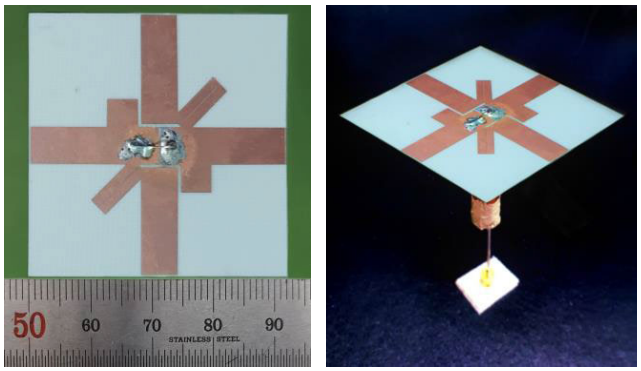

FIGURE 12. Fabricated sample of the uniplanar crossed-dipole antenna: (a) top view and (b) 3-D view.

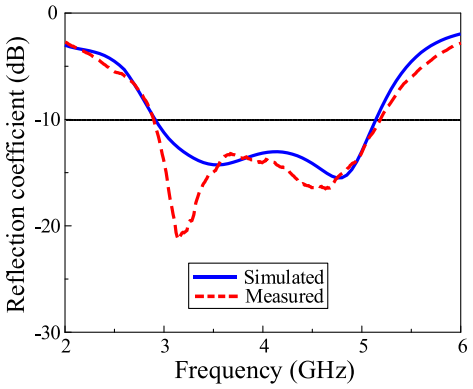

FIGURE 13. Simulated and measured reflection coefficients of the uniplanar crossed-dipole antenna.

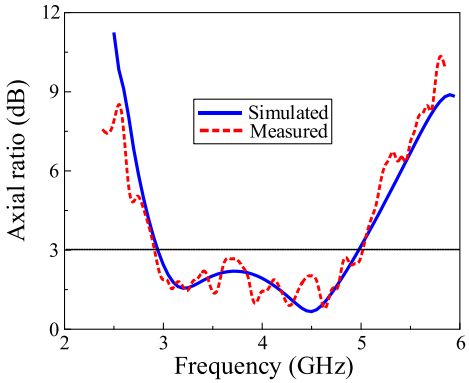

FIGURE 14. Simulated and measured axial ratios of the uniplanar crossed-dipole antenna.

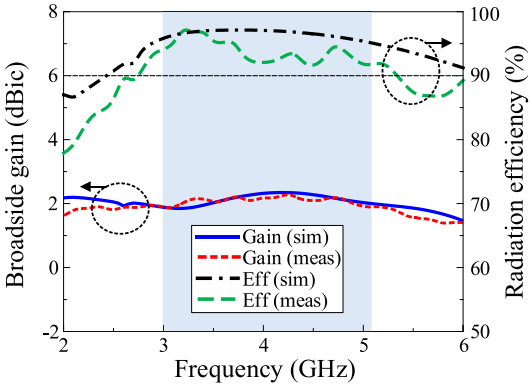

FIGURE 15. Simulated and measured gains and radiation efficiencies of the uniplanar crossed-dipole antenna.

of an additional resonant mode. A multi-layer structured crossed-dipole antenna with an inductive grid metasurface has also been reported [35]. The radiating element consists of a crossed Egyptian axe dipole printed on the top of the dielectric substrate and an L-shaped driven dipole printed on the bottom of the dielectric substrate. An additional resonance mode was made possible by adding an inductive grid metasurface to the radiating element. Although the proposed antenna is small in size, it is difficult to fabricate because it has a multi-layer structure, and the bandwidth of the radiating element is narrow. Thus, there is a limit to the bandwidth expansion of the antenna. In addition, the radiation efficiency of the antenna is as low as 80%. In the proposed antenna, the dipoles constituting the crossed dipole have a wide impedance bandwidth, unlike existing antennas. As a result, a very wide AR bandwidth can be achieved with a simple uniplanar structure, without an additional radiator, and the radiation efficiency is high.

IV. MEASUREMENT RESULTS

The optimized antenna with a balun was fabricated, and its performance was evaluated. Fig. 12 shows the fabricated crossed-dipole antenna printed on the same plane of a thin RO4003 dielectric substrate via the standard wet-etching technology. An Agilent E8362B network analyzer and a 3.5 mm coaxial calibration standard (GCS35M) were used to measure the reflection coefficient. The measured and simulated $|S_{11}|$ were in good agreement, as shown in Fig. 13. Both the simulated and measured $|S_{11}|$ show that there are two resonant modes and that –10 dB impedance bandwidth is almost the same. The measured impedance bandwidth for $|S_{11}| < -10$ dB was 2.91–5.17 GHz (55.94%), and the simulated impedance bandwidth was 2.92–5.15 GHz (55.26%).

Far-field radiation measurements were obtained in a full anechoic chamber with dimensions of 5.5 m (W) × 5.5 m (L) × 5.0 m (H) at the Electromagnetic Wave Technology Institute at Yongsan, Korea. The fabricated antennas were used for receiving, and a standard wideband horn antenna was used for transmitting. The distance between the transmitter and receiver was 2.9 m. The fabricated antenna was rotated from −180° to 180° at a scan angle of 1° and speed of 3° s−1, while the horn antenna was fixed.

The AR was measured at several frequency points, as shown in Fig. 14. The simulated and measured AR are almost identical. The measured and simulated AR bandwidths range from 2.96 GHz to 5.12 GHz (53.5%) and

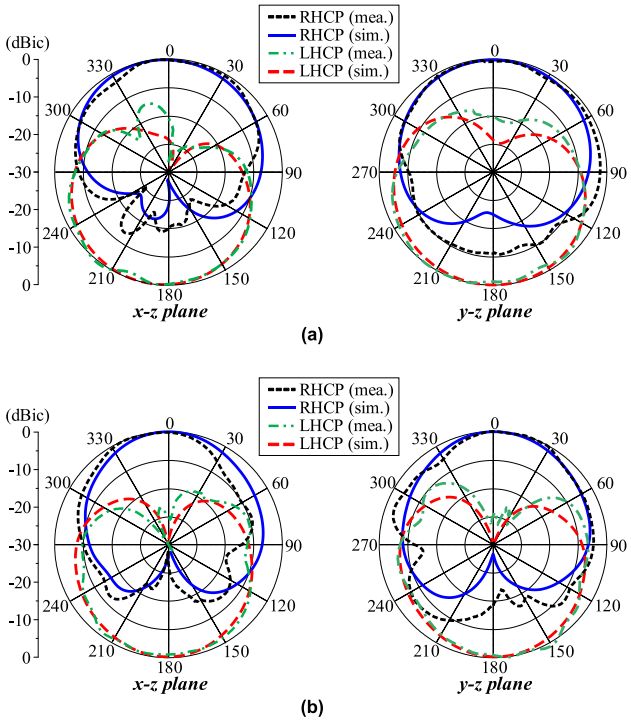

FIGURE 16. Simulated and measured radiation patterns of the uniplanar crossed-dipole antenna: (a) 3.3 GHz and (b) 4.7 GHz.

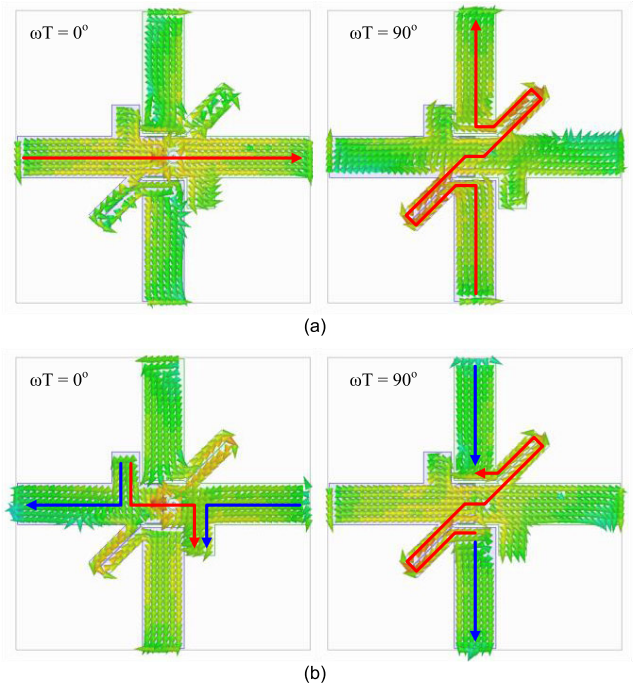

FIGURE 17. Antenna current distributions at each AR minimum point: (a) 3.3 GHz and (b) 4.6 GHz.

from 3.0 GHz to 5.09 GHz (51.7%), respectively. The measured and simulated broadside gains exhibit similar profiles, albeit with small fluctuations resulting from the fabrication imperfections and the foams, racks, and tape used in the measurement setup and mechanical vibrations that occurred during the measurement. The measured gain has a peak value of 2.2 dBic, as shown in Fig. 15. The measured radiation efficiency of the proposed antenna is as high as 93% or more within the operation bandwidth. The radiation patterns measured at the two AR minimum points of 3.3 GHz and 4.6 GHz are shown in Fig. 16. Satisfactory broadside bidirectional CP radiation patterns are obtained. The measured radiation patterns in both the xz- and yz-planes are symmetric and similar to the simulated radiation patterns. The measured radiation patterns exhibit low cross-polarization levels. The measured half-power beamwidths are 117.77° and 129.09° in the xz- and yz-planes at 3.3 GHz, respectively, and 98.76° and 155.95° in the xz- and yz-planes at 4.6 GHz, respectively.

Fig. 17 shows the surface current distribution at two AR minimum point frequencies of the proposed antenna. Fig. 17(a) shows the antenna surface current distribution at 3.3 GHz, the first AR minimum point, and shows that each dipole constituting the crossed-dipole antenna is an RHCP antenna operating in first-order mode. Fig. 17(b) shows the antenna surface current distribution at the second AR minimum point, 4.6 GHz. Unlike the first AR minimum point, the surface current distribution at the second AR minimum point shows that each dipole of the crossed dipole operates in third-order mode.

V. CONCLUSION

A uniplanar crossed-dipole antenna consisting of a pair of folded striplines and stubs is developed. The proposed antenna differs from the existing crossed-dipole antennas in that both the crossed-dipole arms are printed on the same plane of the substrate. Folded striplines are used to connect the dipole arms for CP generation, whereas stubs are designed for impedance matching and AR bandwidth broadening. The antenna produces two resonances in the reflection coefficient profile and two AR bands that are combined to achieve wideband characteristics. The wideband properties of the antenna are numerically and experimentally verified to validate the antenna design. The simulated and measurement results of the proposed antenna are consistent. The antenna exhibits more than 93% radiation efficiency within its AR bandwidths. Its small size, uniplanar configuration, and wideband CP characteristics render the proposed antenna a suitable candidate for wireless communication systems. In addition, as the proposed antenna has a uniplanar structure, only one side of the dielectric substrate is used. Therefore, structures, such as parasitic elements or metasurfaces, can be applied to the other side of the dielectric substrate, and an additional resonant mode can be added without the need for a multi-layered structure.

ACKNOWLEDGMENT

The authors would like to thank Kedze for his helpful comments on various crossed dipole antenna design issues.

REFERENCES

[1] S. Gao, Q. Luo, and F. Zhu, *Circularly Polarized Antennas*. Hoboken, NJ, USA: Wiley-IEEE Press, 2014.

[2] H. Wang, Y. B. Park, and I. Park, "Low-profile wideband solar-cell-integrated circularly polarized CubeSat antenna for the Internet of Space things," *IEEE Access*, vol. 10, pp. 61451–61462, 2022.
[3] Y. Sung, "A dual orthogonal fed monopole antenna for circular polarization diversity," *J. Electromagn. Eng. Sci.*, vol. 22, no. 3, pp. 283–290, May 2022.
[4] K. E. Kedze, H. Wang, and I. Park, "A metasurface-based wide-bandwidth and high-gain circularly polarized patch antenna," *IEEE Trans. Antennas Propag.*, vol. 70, no. 1, pp. 732–737, Jan. 2022.
[5] C. H. S. Nkimbeng, H. Wang, and I. Park, "Coplanar waveguide-fed bidirectional same-sense circularly polarized metasurface-based antenna," *J. Electromagn. Eng. Sci.*, vol. 21, no. 3, pp. 210–217, Jul. 2021.
[6] B. Yen Toh, R. Cahill, and V. F. Fusco, "Understanding and measuring circular polarization," *IEEE Trans. Educ.*, vol. 46, no. 3, pp. 313–318, Aug. 2003.
[7] H. Wang and I. Park, "Compact wideband circularly polarized dipole antenna using modified quadrature hybrid couplers," *IEEE Trans. Antennas Propag.*, vol. 69, no. 12, pp. 8896–8901, Dec. 2021.
[8] H. Hung Tran and I. Park, "Compact wideband circularly polarised resonant cavity antenna using a single dielectric superstrate," *IET Microw., Antennas Propag.*, vol. 10, no. 7, pp. 729–736, May 2016.
[9] S. X. Ta and I. Park, "Compact wideband sequential-phase feed for sequentially rotated antenna arrays," *IEEE Antennas Wireless Propag. Lett.*, vol. 16, pp. 661–664, 2017.
[10] D. Zheng, Y. Luo, and Q. Chu, "Cavity-backed self-phased circularly polarized multidipole antenna with wide axial-ratio beamwidth," *IEEE Antennas Wireless Propag. Lett.*, vol. 16, pp. 1998–2001, 2017.
[11] Y. Luo, Q. Chu, and L. Zhu, "A miniaturized wide-beamwidth circularly polarized planar antenna via two pairs of folded dipoles in a square contour," *IEEE Trans. Antennas Propag.*, vol. 63, no. 8, pp. 3753–3759, Aug. 2015.
[12] J. S. Park, J. H. Hong, and K. W. Kim, "Design of 24–40 GHz ultra-wideband circularly polarized monopole antenna with a defected ground plane," *J. Electromagn. Eng. Sci.*, vol. 22, no. 3, pp. 379–385, May 2022.
[13] S. X. Ta, I. Park, and R. W. Ziolkowski, "Crossed dipole antennas: A review," *IEEE Antennas Propag. Mag.*, vol. 57, no. 5, pp. 107–122, Oct. 2015.
[14] G. Brown, "The turnstile," *Electronics*, vol. 9, pp. 14–17, Apr. 1936.
[15] M. F. Bolster, "A new type of circular polarizer using crossed dipoles," *IEEE Trans. Microw. Theory Techn.*, vol. MTT-9, no. 5, pp. 385–388, Sep. 1961.
[16] K. Maamria and T. Nakamura, "Simple antenna for circular polarisation," *IEE Proc. H Microwaves, Antennas Propag.*, vol. 139, no. 2, pp. 157–158, Apr. 1992.
[17] S. X. Ta, H. Choo, and I. Park, "Planar, lightweight, circularly polarized crossed dipole antenna for handheld UHF RFID reader," *Microw. Opt. Technol. Lett.*, vol. 55, no. 8, pp. 1874–1878, Aug. 2013.
[18] K. E. Kedze, H. Wang, Y. Kim, and I. Park, "Design of a reduced-size crossed-dipole antenna," *IEEE Trans. Antennas Propag.*, vol. 69, no. 2, pp. 689–697, Feb. 2021.
[19] Y. Sun, K. W. Leung, and K. Lu, "Broadbeam cross-dipole antenna for GPS applications," *IEEE Trans. Antennas Propag.*, vol. 65, no. 10, pp. 5605–5610, Oct. 2017.
[20] H. H. Tran, S. X. Ta, and I. Park, "A compact circularly polarized crossed-dipole antenna for an RFID tag," *IEEE Antennas Wireless Propag. Lett.*, vol. 14, pp. 674–677, 2015.
[21] S. X. Ta, K. Lee, I. Park, and R. W. Ziolkowski, "Compact crossed-dipole antennas loaded with near-field resonant parasitic elements," *IEEE Trans. Antennas Propag.*, vol. 65, no. 2, pp. 482–488, Feb. 2017.
[22] Y. He, W. He, and H. Wong, "A wideband circularly polarized cross-dipole antenna," *IEEE Antennas Wireless Propag. Lett.*, vol. 13, pp. 67–70, 2014.
[23] S. X. Ta and I. Park, "Crossed dipole loaded with magneto-electric dipole for wideband and wide-beam circularly polarized radiation," *IEEE Antennas Wireless Propag. Lett.*, vol. 14, pp. 358–361, 2015.
[24] W. Yang, Y. Pan, S. Zheng, and P. Hu, "A low-profile wideband circularly polarized crossed-dipole antenna," *IEEE Antennas Wireless Propag. Lett.*, vol. 16, pp. 2126–2129, 2017.
[25] L. Li, C. Zhang, Y. Shao, and J. Luo, "An SIW-fed cross-dipole antenna with broadband circular polarization for MMW applications," *IEEE Trans. Antennas Propag.*, vol. 70, no. 6, pp. 4830–4835, Jun. 2022.
[26] H. H. Tran, S. X. Ta, and I. Park, "Single-feed, wideband, circularly polarized, crossed bowtie dipole antenna for global navigation satellite systems," *J. Electromagn. Eng. Sci.*, vol. 14, no. 3, pp. 299–305, Sep. 2014.
[27] H. H. Tran and I. Park, "Wideband circularly polarized cavity-backed asymmetric crossed bowtie dipole antenna," *IEEE Antennas Wireless Propag. Lett.*, vol. 15, pp. 358–361, 2016.
[28] J. Baik, T. Lee, S. Pyo, S. Han, J. Jeong, and Y. Kim, "Broadband circularly polarized crossed dipole with parasitic loop resonators and its arrays," *IEEE Trans. Antennas Propag.*, vol. 59, no. 1, pp. 80–88, Jan. 2011.
[29] G. Feng, L. Chen, X. Xue, and X. Shi, "Broadband circularly polarized crossed-dipole antenna with a single asymmetrical cross-loop," *IEEE Antennas Wireless Propag. Lett.*, vol. 16, pp. 3184–3187, 2017.
[30] H. H. Tran, I. Park, and T. K. Nguyen, "Circularly polarized bandwidth-enhanced crossed dipole antenna with a simple single parasitic element," *IEEE Antennas Wireless Propag. Lett.*, vol. 16, pp. 1776–1779, 2017.
[31] W. Yang, Y. Pan, and S. Zheng, "A compact broadband circularly polarized crossed-dipole antenna with a very low profile," *IEEE Antennas Wireless Propag. Lett.*, vol. 18, no. 10, pp. 2130–2134, Oct. 2019.
[32] G. Feng, L. Chen, X. Wang, X. Xue, and X. Shi, "Broadband circularly polarized crossed bowtie dipole antenna loaded with parasitic elements," *IEEE Antennas Wireless Propag. Lett.*, vol. 17, no. 1, pp. 114–117, Jan. 2018.
[33] W. J. Yang, Y. M. Pan, and S. Y. Zheng, "A low-profile wideband circularly polarized crossed-dipole antenna with wide axial-ratio and gain beamwidths," *IEEE Trans. Antennas Propag.*, vol. 66, no. 7, pp. 3346–3353, Jul. 2018.
[34] T. T. Le, Y. Kim, and T. Yun, "Bandwidth-enhanced compact circularly-polarized wearable antenna with a magneto-electric dipole," *IEEE Access*, vol. 10, pp. 123225–123232, 2022.
[35] Q. Lin, M. Tang, M. Li, and R. W. Ziolkowski, "Electrically small, wideband, circularly polarized, inductive grid-array metasurface antenna," *IEEE Trans. Antennas Propag.*, vol. 71, no. 5, pp. 4546–4551, May 2023.
[36] Y. Luo, Z. N. Chen, and K. Ma, "Enhanced bandwidth and directivity of a dual-mode compressed high-order mode stub-loaded dipole using characteristic mode analysis," *IEEE Trans. Antennas Propag.*, vol. 67, no. 3, pp. 1922–1925, Mar. 2019.
[37] Y. Luo, X. Ma, N. Yan, W. An, and K. Ma, "Sidelobe suppression of dual-mode compressed high-order-mode dipole by loading bent stubs," *IEEE Antennas Wireless Propag. Lett.*, vol. 20, no. 6, pp. 898–902, Jun. 2021.
[38] Y. Luo, N. Zhang, Z. N. Chen, W. An, K. Ma, and Q.-X. Chu, "A nonuniform compressed high-order mode dipole with sidelobe suppression," *IEEE Antennas Wireless Propag. Lett.*, vol. 21, no. 12, pp. 2372–2376, Dec. 2022.
[39] S. A. Saario, J. W. Lu, and D. V. Thiel, "Full-wave analysis of choking characteristics of sleeve balun on coaxial cables," *Electron. Lett.*, vol. 38, no. 7, pp. 304–305, Mar. 2002.

HEESU WANG (Graduate Student Member, IEEE) received the B.S. and M.S. degrees in electrical and computer engineering from Ajou University, Suwon, Republic of Korea, in 2018 and 2020, respectively, where he is currently pursuing the Ph.D. degree with the Department of Electrical and Computer Engineering. His research interests include the design of patch antennas, printed antennas, small antennas, and metasurface antennas for various wireless communication applications.

GANGIL BYUN (Senior Member, IEEE) received the B.S. and M.S. degrees in electronic and electrical engineering from Hongik University, Seoul, South Korea, in 2010 and 2012, respectively, and the Ph.D. degree in electronics and computer engineering from Hanyang University, Seoul, in 2015. After his graduation, he returned to Hongik University as a Research Professor and performed active research for two years. In February 2018, he joined the Faculty of Ulsan National Institute of Science and Technology (UNIST), Ulsan, South Korea, where he is currently an Associate Professor with the Department of Electrical Engineering. His principal research areas are in the design and analysis of small antenna arrays for adaptive beamforming applications, such as direction-of-arrival estimation, interference mitigation, and radar. He has actively contributed to the improvement of overall beamforming performances by combining both antenna engineering and signal processing perspectives. His recent research interests include Huygens' metasurface, optically invisible antennas, electromagnetic sensors, and waveguide slot array antennas to bring advances in future wireless communication systems.

YONG BAE PARK (Senior Member, IEEE) received the B.S., M.S., and Ph.D. degrees in electrical engineering from the Korea Advanced Institute of Science and Technology, South Korea, in 1998, 2000, and 2003, respectively. From 2003 to 2006, he was with the Korea Telecom Laboratory, Seoul, South Korea. In 2006, he joined the School of Electrical and Computer Engineering, Ajou University, South Korea, where he is currently a Professor. His research interests include electromagnetic field analysis, high-frequency methods, metamaterial antennas, radomes, and stealth technology.

IKMO PARK (Member, IEEE) received the B.S. degree in electrical engineering from the State University of New York at Stony Brook and the M.S. and Ph.D. degrees in electrical engineering from the University of Illinois at Urbana–Champaign. In 1996, he joined the Department of Electrical and Computer Engineering, Ajou University. Prior to joining Ajou University, he was with the Device and Materials Laboratory, LG Corporate Institute of Technology, Seoul, Republic of Korea, where he had been engaged in research and development of various antennas for personal communication systems, wireless local area networks, and direct broadcasting systems. He was a Visiting Professor with the Department of Electrical and Computer Engineering, POSTECH, Pohang, Republic of Korea, from March 2004 to February 2005, and the Department of Electrical and Computer Engineering, The University of Arizona, Tucson, AZ, USA, from July 2011 to June 2012. He has authored and coauthored more than 400 technical journal and conference papers. He also holds over 50 domestic and international patents. He served as the Chair of the Department of Electrical and Computer Engineering, Ajou University. He is a member of Eta Kappa Nu and Tau Betta Pi. He is also a member of the Board of Directors of the Korea Institute of Electromagnetic Engineering and Science (KIEES). He serves as the Editor-in-Chief for the *Proceedings of the KIEES* and *Journal of KIEES*, an Editorial Board Member for the *International Journal of Antennas and Propagation*, and an Associate Editor for *IET Electronics Letters*. He served as an Editorial Board Member for the *Journal of Electromagnetic Engineering and Science*.